ARTICLE

Cholinergic Modulation of Angiogenesis: Role of the 7 Nicotinic Acetylcholine Receptor

Jenny C.F. Wu,[1] Andrzej Chruscinski,[1,2] Vinicio A. De Jesus Perez,[3] Harvir Singh,[2] Maria Pitsiouni,[1] Marlene Rabinovitch,[3] Paul J. Utz,[2] and John P. Cooke[1]*

[1]*Department of Cardiovascular Medicine, Stanford University, Stanford, California 94305*
[2]*Department of Immunology, Stanford University, Stanford, California 94305*
[3]*Department of Medicine, Stanford University, Stanford, California 94305*

ABSTRACT

Pathological angiogenesis contributes to tobacco-related diseases such as malignancy, atherosclerosis and age-related macular degeneration. Nicotine acts on endothelial nicotinic acetylcholine receptors (nAChRs) to activate endothelial cells and to augment pathological angiogenesis. In the current study, we studied nAChR subunits involved in these actions. We detected mRNA for all mammalian nAChR subunits except α_2, α_4, γ, and δ in four different types of ECs. Using siRNA methodology, we found that the α_7 nAChR plays a dominant role in nicotine-induced cell signaling (assessed by intracellular calcium and NO imaging, and studies of protein expression and phosphorylation), as well as nicotine-activated EC functions (proliferation, survival, migration, and tube formation). The α_9 and α_7 nAChRs have opposing effects on nicotine-induced cell proliferation and survival. Our studies reveal a critical role for the α_7 nAChR in mediating the effects of nicotine on the endothelium. Other subunits play a modulatory role. These findings may have therapeutic implications for diseases characterized by pathological angiogenesis. J. Cell. Biochem. 108: 433–446, 2009.   © 2009 Wiley-Liss, Inc.

KEY WORDS: nAChR; siRNA; RPP

Several years ago we serendipitously discovered that nicotine promotes pathological angiogenesis [Heeschen et al., 2001]. This unexpected finding is significant because many tobacco-related diseases, such as malignancy, rheumatoid arthritis, atherosclerosis, and retinopathy, are characterized by pathological angiogenesis [Folkman, 1995; Cooke, 2007]. Our subsequent work using preclinical models indicates that nicotine (as a chemical, or as in second hand tobacco smoke) stimulates angiogenesis during inflammation, ischemia, tumorigenesis, and atherogenesis [Heeschen et al., 2001, 2002; Zhu et al., 2003]. Most recently, in an animal model of age-related macular degeneration (AMD), we find that nicotine accelerates the choroidal neovascularization that is characteristic of this condition [Kiuchi et al., 2008]. The angiogenic action of nicotine (or second hand smoke) is mediated at least in part by nicotinic acetylcholine receptors (nAChR) in endothelial cells

[Cooke, 2007]. Indeed, antagonists which are broadly active against nAChRs (such as mecamylamine or hexamethonium ion) inhibit the angiogenic effects of nicotine (or second hand smoke) in vitro and in vivo [Heeschen et al., 2002].

The nAChR is a ligand gated cationic channel. The receptor is a pentameric protein consisting of combinations of 16 isoforms of subunits including α subunits (α_1–α_{10}), β subunits (β_1–β_4), γ, δ, and/or ε subunits [Gotti et al., 2007]. Most nAChRs are heteromers composed of a combination of α and β subunits, and are primarily permeable to sodium and potassium. The heteromeric nAChR of the neuromuscular junction is composed of α_1, β_1, δ, and ε subunits, and is also permeable to monovalent cations. By contrast, the α_7 and α_9 are unique in their ability to form functional homomeric receptors [Boulter et al., 1987; Elgoyhen et al., 1994; Lips et al., 2002], and are more permeable to calcium than to monovalent cations.

In the central nervous system, the combinatorial association of different α- and β-subunits gives rise to diversity in both structure and function, with receptors of different channel properties and signaling patterns. Approximately 10 years ago, nAChRs were discovered outside of the central nervous system [as reviewed in Grando et al., 2007]. Much less is known about the distribution and signaling of these non-neuronal nAChRs.

The purpose of this study was to characterize the endothelial nAChR subunits in EC, and to elucidate their role in mediating the angiogenic response to nicotine. We examined the role of nAChRs in several angiogenic processes including EC migration, proliferation and tubulogenesis. To link these functional responses to specific nAChR subunit expression, we inhibited the expression of nAChR subunits using small interfering RNA (siRNA). We report that the α_7 nAChR plays a critical role in nicotine signaling and angiogenic processes. Of interest, we find that the α_9 nAChR opposes the effects of the α_7 nAChR upon cell proliferation and apoptosis. The distinctive roles for α_7 and α_9 nAChRs is reflected by the divergent phosphoproteomic profiles induced by their siRNA suppression.

RESULTS

EXPRESSION OF nAChR SUBUNITS IN ECs

We identified the nAChR subunits present in four human endothelial cell types: human pulmonary arterial endothelial cells (HPAEC), human dermal microvascular endothelial cells (HMVEC), human umbilical vein endothelial cells (HUVEC), and human retinal endothelial cells (HREC) by performing nAChR subunit-specific RT-PCR analysis for the nAChR subunits known to be expressed in adult humans, α_{1-7}, α_9, α_{10}, β_{1-4}, δ, and ϵ (the γ subunit is not expressed in the adult, and the α_8 subunit is avian). We detected endothelial mRNA for each of the known mammalian nAChR subunits with the exception of α_2, α_4, γ, and δ in the four different types of endothelial cells. There are differences in the levels of expression of various nAChR subunits between the cell types (Fig. 1). To assess the significance of the expressed nAChR subunits, we performed an siRNA screen. In these preliminary studies (d.n.s.) we treated ECs with siRNA probes that effectively suppressed mRNA expression of each of the subunits. Subsequently, the effect of these probes (or scrambled siRNA) on EC proliferation was observed, in the presence of vehicle or nicotine 10 nM. These studies indicated that RNAi against α_7 markedly reduced basal and nicotine-induced EC proliferation. By contrast, RNAi against the other subunits either had no effect, or even enhanced basal or nicotine-induced EC proliferation. Notably, siRNA directed against α_9 (the other subunit known to form calcium-selective homomeric channels), appeared to enhance nicotine induced EC proliferation. To focus this investigation, we chose to further study the differences in signaling and functional effects of the two homomeric nAChRs, α_7 and α_9.

ROLE OF α_7 AND α_9 nAChR SUBUNITS IN EC PROLIFERATION AND SURVIVAL

In nanomolar concentrations, nicotine stimulates DNA synthesis and proliferation in ECs in vitro [Villablanca, 1998; Heeschen et al.,
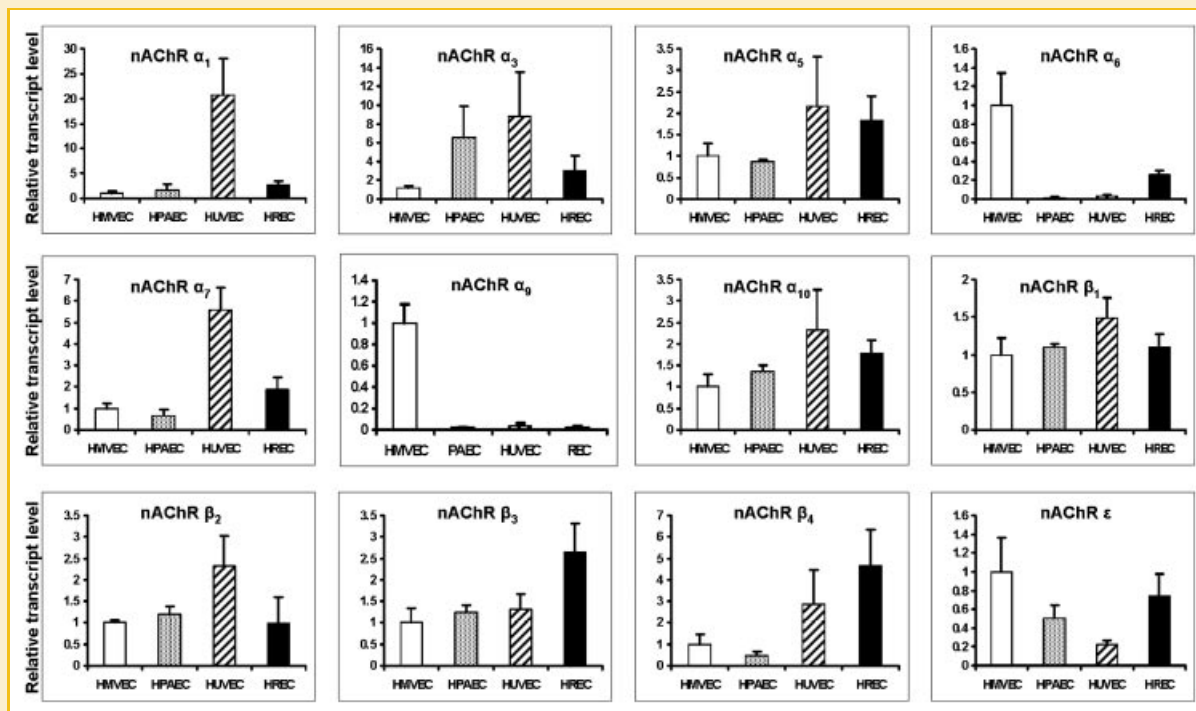

Fig. 1. Endothelial expression of mRNA for nAChR subunits. Gene expression of nAChR subunits in HMVEC, HPAEC, HUVEC and HREC were assessed by Real-time PCR. The c_t values for nAChR subunits were normalized using c_t values obtained in parallel for 18S mRNA. Subsequently, these values were expressed as relative transcript levels by comparison to those values determined for HMVEC. Endothelial mRNA was detected for each of the known mammalian nAChR subunits with the exception of $\alpha2$, $\alpha4$, γ, and δ in each of the four different types of endothelial cells. The data represent the mean of three different experiments carried out in triplicate with error bars showing SEM.

2001; Dasgupta and Chellappan, 2006]. To examine the differing effects of the α_7 and α_9 nAChRs in this response, we transfected EC with siRNA against these specific nAChR subunits. Some monolayers were treated with scrambled siRNA as a control for the transfection. Effective siRNA knockdown of the expression of each nAChR was confirmed by RT-PCR (Fig. 2A) as well as Western analysis (Fig. 2B). We achieved a 70% knockdown of mRNA for a9 nAChR, and an 85% knockdown of mRNA for a7 nAChR. After 72 h of transfection, we exposed the EC to vehicle or nicotine (10^{-10} M). Proliferation was measured by BrdU incorporation assay.

Silencing of the α_7 gene inhibited basal cell growth by 25%, and fully abrogated nicotine-enhanced proliferation (Fig. 2C). By contrast, siRNA silencing of the α_9 gene paradoxically enhanced basal and nicotine-induced proliferation. The results indicated that the α_7 nAChR mediates nicotine-induced EC proliferation, whereas the α_9 nAChR opposes this proliferative influence.

At clinically relevant concentrations, nicotine enhances cell survival [Heeschen et al., 2001]. ECs were serum starved for 24 h and then exposed to vehicle or nicotine (10^{-10} M) for 24 h. Serum starvation induced apoptosis, which was inhibited by nicotine. Knockdown of α_7 gene expression enhanced apoptosis in the absence of nicotine, and abrogated the anti-apoptotic effect of nicotine (Fig. 2D), whereas suppression of the α_9 gene had little effect. The findings confirmed that the α_7 nAChR is required for nicotine-induced EC survival.

ROLE OF nAChR SUBUNITS IN EC MIGRATION

We subsequently assessed the roles of the two homomeric receptors in nicotine-induced EC migration in HMVEC. Nicotine stimulates EC migration in a dose-dependent manner, an effect which is blocked by pharmacological antagonists of the nAChR. After wounding of the monolayer, cells were treated with vehicle, nicotine or VEGF. VEGF was used here as a positive control for EC migration. Twelve hours after wounding, the HMVEC migration into the denuded area was assessed (Fig. 3A). Nicotine (10 nM) promoted EC migration (1.8-fold vs. control, $P < 0.001$; Fig. 3B). We have previously reported that VEGF is a more potent migragen than nicotine or FGF in this assay [Ng et al., 2007]. In the current study, EC migration in response to VEGF (10 ng/ml) tended to be greater than that to nicotine. Knockdown of α_9 nAChR expression had no qualitative effect on nicotine-stimulated EC migration. However, siRNA against α_7, significantly reduced the effect of nicotine to induce EC migration (Fig. 3B). The results indicate that the α_7 nAChR plays a dominant role in nicotine-induced EC migration.

Intriguingly, VEGF-induced EC migration was also blunted by siRNA against α_7 but not α_9 nAChR message (Fig. 3B). This finding is consistent with our previous observation that pharmacological antagonism of the nAChR attenuates VEGF-induced EC migration [Ng et al., 2007]. These observations and our previous work indicate an interdependence of the angiogenic pathways mediated by the VEGFR and the nAChR [Ng et al., 2007].

OPPOSING EFFECTS OF nAChR SUBTYPES ON EC TUBE FORMATION

Endothelial cells plated on Matrigel proliferate, migrate and differentiate into networks of endothelial tubes, modeling angiogenesis. Nicotine enhances tube formation in Matrigel [Heeschen

et al., 2001], which we confirmed in the current study (Fig. 4A). Suppression of the α_9 nAChR gene had little or no effect on tube formation (Fig. 4B). Conversely, basal as well as nicotine-induced tube formation was inhibited by silencing expression of the α_7 gene (Fig. 4B). Basal tube formation is under control of existing growth factors in the Matrigel, including VEGF. The effect of α_7 siRNA to inhibit basal tube formation is again consistent with an interdependency of VEGFR and nAChR stimulation of angiogenic processes.

ROLE OF nAChR SUBTYPE ON Ca^{2+} INFLUX

By contrast with the heteromeric nAChRs (which are permeable to monovalent cations), the homomeric nAChRs composed of α_7 or α_9 subunits, are calcium permeable channels in the brain [Fucile, 2004]. To determine the role of α_7 or α_9 subunits in nicotine-induced calcium mobilization in the endothelium, we combined the siRNA approach described above with Ca^{2+} imaging using fluo-4 and fluorescence microscopy. Nicotine induced a transient elevation of cytoplasmic Ca^{2+}, an effect that was markedly inhibited by siRNA to reduce gene expression of α_7, but not α_9 nAChRs (Fig. 5A,B; Ca^{2+} relative fluorescence intensity in α_7 siRNA treated cells, 78.2 ± 35.8, vs. control cells, 249.8 ± 15.2, $P < 0.001$). The results indicate that the α_7 nAChR mediates nicotine-induced Ca^{2+} mobilization in ECs.

α_7 IS NECESSARY FOR NICOTINE-INDUCED ACTIVATION OF β-CATENIN

The intracellular signaling protein and transcriptional activator β-catenin regulates acetylcholine receptor clustering in muscle cells through its interaction with rapsyn [Zhang et al., 2007]. We were interested to know if β-catenin might be involved in EC nAChR signaling. Immunohistochemistry of unstimulated human dermal microvascular endothelial cells (HMVEC) revealed that β-catenin was primarily associated with the intercellular junctions (Fig. 6A, upper left panel). Upon EC stimulation with nicotine (10^{-8} M), β-catenin became redistributed to the cytoplasm and nucleus (Fig. 6A, upper right panel). Silencing of α_7 nAChR gene expression had no effect on basal level of β-catenin (Fig. 6A, middle left panel), but it largely abolished nicotine-induced accumulation of β-catenin in the cytoplasm and nucleus (Fig. 6A, middle right panel), a finding which was confirmed by immunoblotting (Fig. 6B) with an antibody against β-catenin. These observations were confirmed using an antibody that recognizes the active non-phosphorylated forms of β-catenin (Fig. 6C,D). By contrast, suppression of α_9 nAChR gene expression did not reduce basal or nicotine-induced β-catenin expression and activity. Taken together, these observations indicate that nicotine induces β-catenin activity, an effect that is mediated in large part by the α_7 nAChR.

β-Catenin serves as a transcription cofactor by interacting with T-cell factor (TCF)/lymphocyte enhancer factor to regulate gene expression in the Wnt/β-catenin pathway [Behrens et al., 1996; Ilan et al., 2003]. Accordingly, we used a TCF reporter construct to confirm the importance of the α_7 nAChR in nicotine-induced β-catenin activity. The TOPflash reporter construct consists of six tandem TCF binding sites upstream of a TK promoter driving the firefly luciferase gene. HMVEC were first transfected with siRNA-α_7 followed 24 h later by transfection of the TOPflash reporter. The
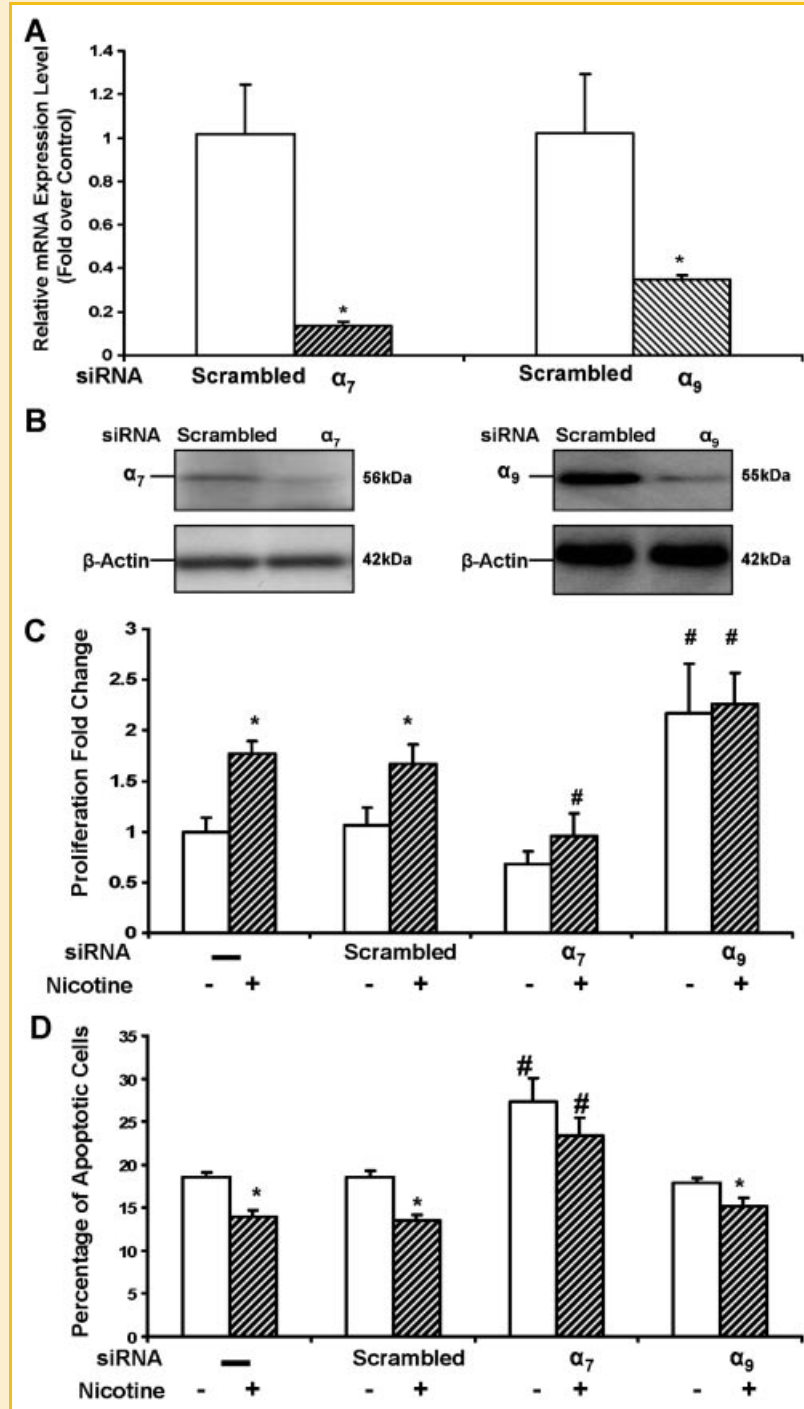
Fig. 2. nAChR mediated endothelial cell proliferation and survival. To assess the role of the homomeric nAChRs in EC proliferation and survival, siRNA methodology was employed. HMVEC were transfected with siRNA against the α_7 or α_9 nAChR subunits or scrambled siRNA or exposed to transfection vehicle without siRNA, for 72 h. A: Gene silencing of the specific nAChR was validated by RT-PCR. Total RNA was isolated and subjected to RT-PCR. The data represent three different experiments carried out in triplicate. The values are expressed as relative fold change of each condition versus control without siRNA with error bars showing SEM ($P < 0.05$). B: Gene silencing of the specific nAChR was validated by Western immunoblots for α_7 or α_9 nAChR and β-actin expression. C: Effect of siRNA on EC proliferation. The proliferation assay utilized BrdU incorporation. Nicotine stimulated HMVEC proliferation, an effect that was abrogated by siRNA against α_7 nAChR. By contrast, siRNA against α_9 nAChR increased basal EC proliferation. Results are shown as fold change (mean ± SEM of three different experiments each carried out in triplicate) compared to the nonstimulated control cells. $^*P < 0.001$ vehicle versus nicotine treated cells. $^\#P < 0.05$, versus non-transfected cells exposed to same stimulus. D: Effect of siRNA on EC survival. Cells were first transfected with siRNA as described in (A). Subsequently, serum free conditions were used to induce apoptosis for 24 h, then either vehicle or nicotine(10^{-10} M) was added to the medium and the cells were further cultured for another 24 h. The cell survival assay is described in Materials and Methods Section. $^*P < 0.05$ vehicle versus nicotine treated cells. $^\#P < 0.05$ versus non-transfected cells exposed to same stimulus.
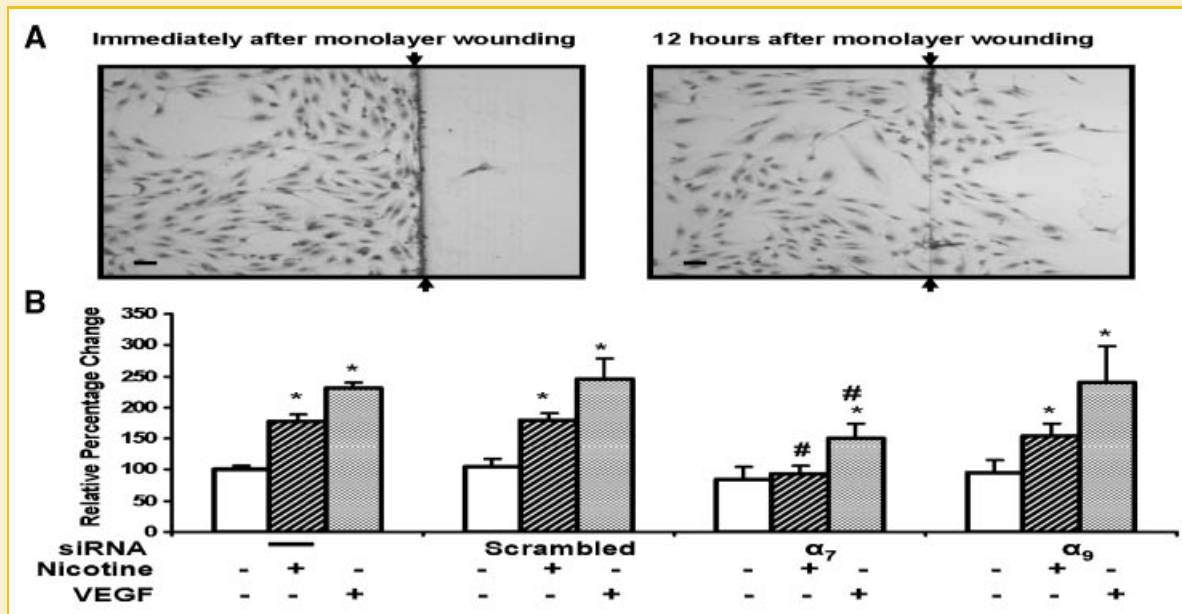
Fig. 3. Role of nAChR subunits in human microvascular EC migration. A: Representative microphotographs of the HMVEC migration assay. Nicotine (10^{-8} M) stimulates migration of HMVEC into denuded area (right panel). Bar = 50 μm. B: Effect of silencing individual nAChR on HMVEC migration induced by nicotine (10^{-8} M), or VEGF (10 ng/ml). Endothelial cells exposed to scrambled siRNA were used as a control for the effects of transfection. Values are expressed as a percentage of migrating cells per high-powered field (n = 12) in vehicle-treated wells with error bars showing SEM. $^{**}P < 0.05$ versus vehicle treated cells. $^{#}P < 0.05$, versus non-transfected cells exposed to same stimulus.

FOPflash reporter construct, which carries mutant TCF binding sites, was used as negative control. After 4 h stimulation with nicotine, a 3.5-fold increase in luciferase activity was detected in cultured EC stimulated with nicotine. This nicotine-induced activity was reduced by 63% using by siRNA against α_7 ($P < 0.001$, Fig. 6E). A similar effect was observed in human pulmonary arterial endothelial cells (HPAEC) (data not shown). Unexpectedly, we also observed that siRNA against α_9 gene expression blunted nicotine-induced transcriptional activity (though not to the same degree as knockdown of α_7 gene expression. In view of the lack of effect of α_9 siRNA on beta catenin activity, these studies indicate that the α_9 nAChR may enhance the activity of the TCF promoter via a mechanism not dependent upon β-catenin.

PHOSPHOPROTEIN PROFILING OF NICOTINE SIGNALING

To further our understanding of the signaling of nAChRs in endothelial cells, we utilized reverse phase protein (RPP) microarrays developed at Stanford [Chan et al., 2004]. The RPP microarray allows for the simultaneous measurement of the phosphate status of multiple signaling proteins [Chan et al., 2007]. We focused on phosphoproteins representative of those involved in angiogenic processes including proliferation, survival and migration. HMVEC were transfected with siRNA against gene expression of the α_7 or α_9 nAChR for 72 h, then serum starved overnight and treated with nicotine (10^{-10} M). We harvested lysates at several time points following nicotine treatment. The cell lysates were printed in triplicate on nitrocellulose coated slides to generate microarrays. Microarrays were probed with antibodies directed against specific phosphoproteins, processed and analyzed as described previously

[Chan et al., 2004] (Fig. 7A). To compensate for variations during spotting and sample preparation, we normalized the signal intensity of each spot to the level of β-actin, which serves as an internal marker for the total protein deposited.

Figure 7A shows an image of a typical RPP microarray. Figure 7B shows a hierarchical clustering analysis with time course data from control ECs or ECs treated with siRNA against α_7 or α_9 nAChR subunits. Nicotine induced phosphorylation of Raf-1, MEK, MAPK, ERK, p90RSK, and ELK (Fig. 7B). This is significant because p90RSK and Elk1, are targets of ERK, and play a role in EC proliferation [Fradin and Gammeltoft, 1999].

The activation of the signaling proteins by nicotine was markedly suppressed by siRNA against α_7. By contrast, siRNA against α_9 did not block nicotine-induced phosphorylation. Indeed, siRNA against α_9 appeared to increase basal phosphorylation of several of these proteins (Fig. 7B). To validate the array-determined phosphorylation changes, conventional Western immunoblots were performed for individual phosphoproteins (Fig. 7C,D).

In the RPP microarray studies, we also assessed the kinetics of phosphoproteins involved in EC survival, including Akt, PDK1 and BAD. Nicotine increased Akt phosphorylation at Ser473 and Thr308 in a time- and dose-dependent manner (Fig. 7B). Stimulation of Akt phosphorylation at Ser473 by nicotine was evident within 1 min, with a peak at 30 min. BAD is one of the Bcl2 family members, and phosphorylation negatively regulates its proapoptotic activity. Nicotine induced BAD phosphorylation (Ser112), peaking at 60 min. Of note, the peak in phosphorylation of BAD occurred later than that for Akt(Ser308) (i.e., 60 min vs. 30 min; Fig. 7B). These results suggest that nicotine-induced BAD phosphorylation could be
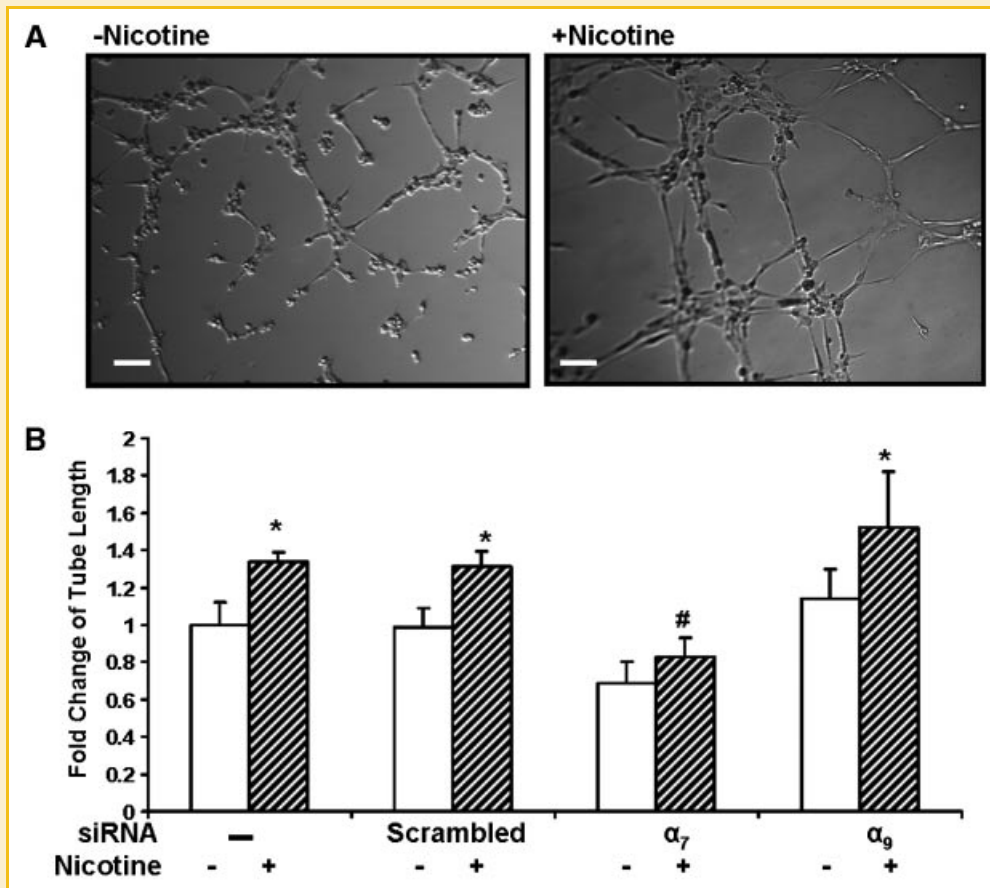
Fig. 4. Role of nAChR subtypes in EC tube formation. A: Representative phase-contrast micrographs of tube formation of HMVECs on Matrigel. HDMECs were pretreated with siRNA against each individual nAChR subunit for 72 h. The cells were seeded on matrigel and incubated at 37°C for 6 h in medium with vehicle (left panel) or with nicotine (10^{-8} M, right panel). Bar, 100 μm. B: Relative fold change in tube length compared to vehicle treated cells. $^*P < 0.05$ versus vehicle treated cells. $^#P < 0.05$ versus non-transfected cells exposed to same stimulus.

mediated by Akt, and/or induction of gsk3β/cyclin D1 signaling [Datta et al., 1999; Hay, 2005]. Silencing of the α_7 but not the α_9 nAChR gene, abolished these nicotine-induced activation patterns. These studies are concordant with our other data indicating the primacy of the α_7 nAChR in mediating the EC response to nicotine.

SIGNALING MECHANISMS MEDIATING NICOTINE-INDUCED NO PRODUCTION

Endothelium derived nitric oxide (NO) plays a key role in angiogenic response [Shesely et al., 1996; Cooke and Losordo, 2002], and NO synthase activity is increased by Akt-mediated phosphorylation at Ser1177 [Dimmeler et al., 1999]. We observed that nicotine increased eNOS phosphorylation, an effect which was antagonized by α_7 but not α_9 siRNA (Fig. 7B). To confirm these findings, we assessed NO elaboration from cultured cells using an NO-sensitive indicator (4-amino-5-methyl-amino-2′,7′-difluorofluorescein diacetate, DAF-FM DA) [Kojima et al., 1998] imaged by inverted microscopy and a CCD digital camera. Nicotine induced a signal within a 15 min (Fig. 8A), and increased NO levels by 4.5-fold in HMVECs ($P < 0.005$ vs. untreated cells). This effect of nicotine was almost abrogated by siRNA against the α_7 nAChR gene (70%

reduction vs. cells treated with transfection vehicle only, $P < 0.001$). By contrast, siRNA against the α_9 nAChR increased NO synthesis at the 1 min time point (Fig. 8B). As expected, the PI$_3$K inhibitor, LY294002 (50 μM), and the MAPK inhibitor U0126 (20 μM; Fig. 8A,C) significantly reduced NO production. Taken together, these results indicate that nicotine increases eNOS phosphorylation and activity, an effect that is mediated in large part by the α_7 nAChR.

nAChR ON CELL CYCLE REGULATION PROTEINS

To characterize intermediate endpoints that may be associated with nicotine-induced activation of endothelial cell proliferation, we examined the expression of cell cycle regulation proteins cyclin D1 and p21Waf1/Cip1 [Obaya and Sedivy, 2002]. ECs were transfected with siRNA-α_7, siRNA-a$_9$ or scrambled siRNA for 72 h and subsequently incubated with nicotine (10^{-10} M) for 24 h. Cell lysates were harvested and subjected to immunoblot analysis. Nicotine inhibited the expression of p21 whereas it increased cyclin D1 by over twofold ($P < 0.005$ vs. untreated cells). The effect of nicotine was on cyclin D1 was nearly abolished by siRNA against α_7 (Fig. 9). By contrast, siRNA against α_9 increased the basal level of cyclin D1 (1.4-fold, $P < 0.005$).
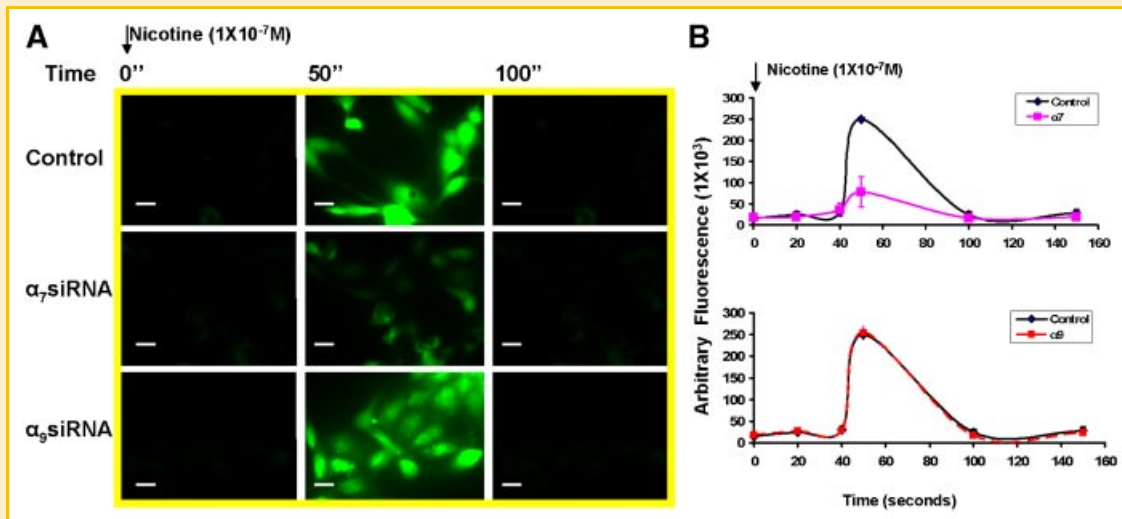
Fig. 5. Nicotine increases intracellular Ca^{2+}. A: Fluorescence photomicrograph of HMVEC cells loaded with fluo-4. Nicotine (10^{-7} M) elevated intracellular Ca^{2+} as indicated by increase in fluorescence emission intensity: left panels (before stimulation) middle panels (50 s after stimulation), and right panels (100 s after stimulation). Upper row: control cells; middle row: middle row: response of cells previously exposed to siRNA against α_7 for 72 h; bottom row: response of cells previously exposed to siRNA against α_9 for 72 h. A representative photomicrograph is shown. Bar, 10 μm. B: Time course of fluorescence emission intensity in HMVEC cells loaded with fluo-4. Cell were transfected and stimulated as described in (A). The values are expressed as arbitrary fluorescence intensity. The average of 10 measurements (without baseline subtraction) in the assay was plotted. [Color figure can be viewed in the online issue, which is available at www.interscience.wiley.com.]

DISCUSSION

In this study, we have characterized the expression of nAChR subunits in several types of human endothelial cells. Although there is type-specific expression of nAChR subunits, the α_7 nAChR subunit is expressed in all EC types. Using siRNA methodology, and employing multiple cell biological, molecular and biochemical endpoints, we find that the α_7 nAChR subunit is of major importance in mediating the effects of nicotine on endothelial cells. Nicotine-induced EC proliferation, survival, migration and tube formation was abrogated or severely attenuated after downregulation of the α_7 nAChR subunit. Depending upon the cell type and process considered, other nAChR subunits may modulate or even oppose the action of the α_7 nAChR. Indeed, there are some intriguing differences between the actions of the two homomeric receptors, the α_7 and the α_9 nAChR.

The heteromeric neuronal receptors, and the nAChR in the neuromuscular junction, are more permeable to the monovalent cations sodium and potassium. By contrast, the homomeric α_7 nAChR is preferentially permeable to calcium. Accordingly, we examined the effect of nicotine upon intracellular levels of calcium, and the role of the α_7 nAChR. Nicotine increased intracellular calcium, an effect that was almost abolished by suppression of α_7 nAChR expression. By contrast, siRNA downregulation of the α_9 nAChR had no effect on nicotine-induced elevation of intracellular calcium.

Intracellular calcium activates kinases involved in EC proliferation, survival and migration. In nanomolar concentrations (a clinically relevant concentration range), nicotine activated Raf-1, MEK, MAPK, ERK, p90RSK, and ELK in a time-dependent fashion. This kinase cascade modulates the expression of cell cycle proteins such as cyclin D1 and p21. A burst of cyclin D1 synthesis occurs every time a cell enters G1 after growth factor stimulation, whereas in quiescent cells, cyclin D1 is inhibited by cdk inhibitor p21 [Morgan, 1995]. Nicotine increased expression of cyclin D, and attenuated the expression of p21, consistent with its growth promoting effects on EC. Furthermore, nanomolar concentrations of nicotine increased EC survival, an effect associated with upregulation of Akt and downregulation of BAD activity, as well as increased synthesis of NO (a major determinant of EC survival and mitogenesis). Most notably, we observed that the effects of nicotine to promote kinase cascades involved in EC proliferation and survival were abrogated by siRNA against α_7, but not α_9 nAChR gene expression.

The major endothelial adhesive protein, VE-cadherin, is linked to the actin cytoskeleton in association with β-catenin [Guo et al., 2004]. Tyrosine phosphorylation of both VE-cadherin and β-catenin disrupts their binding, with consequent nuclear translocation of β-catenin. This step is important in disassembly of endothelial adherens junctions, and precedes EC migration [Dejana, 2004]. We detected β-catenin by immunohistochemistry at the intercellular junctions of endothelial cells. Nicotine caused a rapid redistribution of β-catenin to the nucleus. This observation suggests that β-catenin may mediate some of the transcriptional effects of nicotine. Indeed, in a promoter construct assay, we confirmed nicotine-induced transcriptional activation via β-catenin. These effects of nicotine on β-catenin were abrogated by downregulation of the α_7 nAChR.

Recently, Barbieri et al. [2008] found that tobacco smoke induced β-catenin redistribution to the nucleus in endothelial cells, an effect that was enhanced by IL-1 β. The authors did not determine if nicotine mediated this effect. However, they documented that the
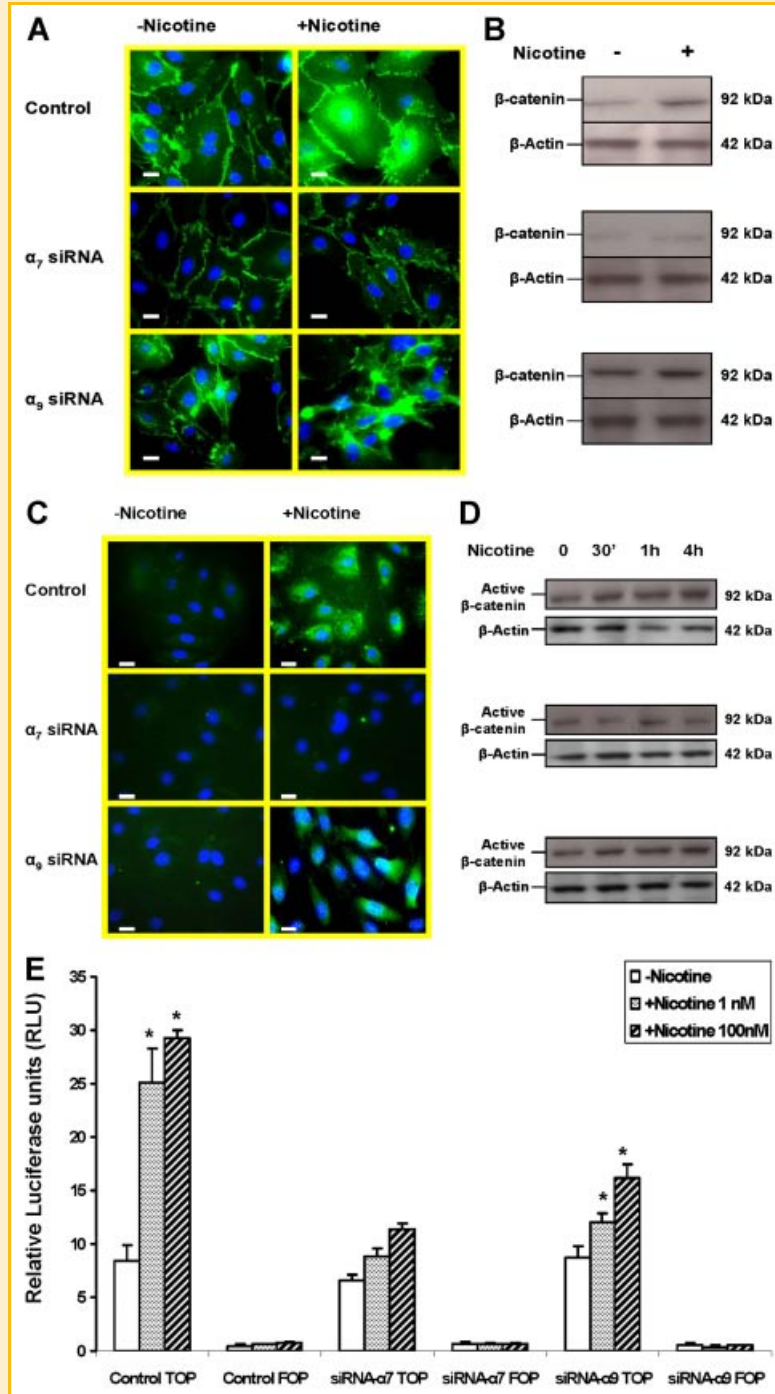
Fig. 6. The α_7 nAChR is necessary for nicotine–induced activation of β–catenin. A: In untreated HMVEC (upper left panel) β–catenin was immunolocalized to the membrane; HMVEC exposed to nicotine (10^{-8} M) for 24 h manifested an increase in β–catenin in the cytoplasm and nucleus (upper right panel); HMVEC were exposed to transfection vehicle (upper panels) or transfected with siRNA against α_7 (middle panels) or α_9 (bottom panels) for 72 h and then exposed to vehicle (left panels) or to 10^{-8} M nicotine (right panels) for 24 h. Hoechst staining (blue) for nuclei, and FITC staining for β–catenin (green). Bar $= 5\,\mu$m. B: Representative Western immunoblots for β–catenin and β–Actin in response to nicotine stimulation for 24 h in control cells, siRNA–α_7 transfected cells, and siRNA–α_9 transfected cells. C: Active β–catenin accumulation in both nuclei and cytoplasm were observed by immunofluorescence 4 h after stimulation by nicotine (10^{-8} M) in control and siRNA–α_9 transfected cells, but not siRNA–α_7 transfected cells. D: Immunoblotting for active β–catenin showed an increase which peaked 30 min after nicotine stimulation, an effect that was blocked by siRNA against α_7 but not α_9 nAChR gene expression. E: Effect of nicotine on T-cell factor (TCF) activity. HMVEC were transfected, siRNA against α_7 or α_9 or with scrambled siRNA for 48 h and subsequently transfected with TOPflash, a TCF–responsive firefly luciferase reporter plasmid for another 24 h. Some cells were transfected with FOPflash, which contains mutant TCF binding sites, for use as a negative control. Cells were also transfected with pRL–TK, a *Renilla* luciferase plasmid which was used for normalization of transfection efficiency. Luciferase activity was analyzed 4 h after addition of nicotine to the cells. Values are TOPflash RLUs from three different experiments. Error bars represent mean $\pm$ SEM, *$P < 0.05$ versus unstimulated control. [Color figure can be viewed in the online issue, which is available at www.interscience.wiley.com.]
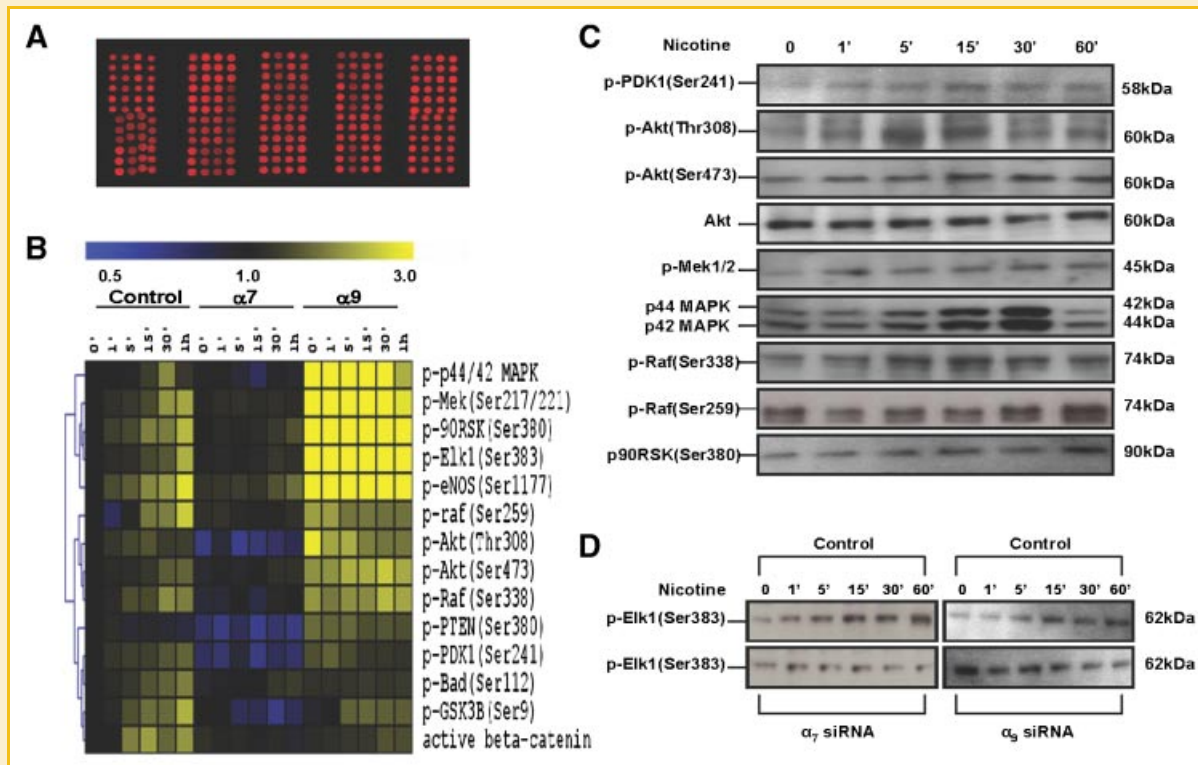
Fig. 7. Reverse phase protein (RPP) microarray profiling of nicotine stimulated ECs. A: Lysates derived from control cells or cells pretreated with siRNA against each nAChR subunit were quantified by protein amount and printed on nitrocellulose–coated slides in three triplicates. Fluorescent image of a representative RPP microarray probed with a primary antibody specific for the phospho–c–Raf is shown. Each 4×12 subarray contains lysates derived from a single nAChR knockdown subunit. Each feature on the array is approximately 400 μm in diameter. B: Hierarchical cluster analysis of phosphorylation protein kinetics effects of nicotine in HMVECs. The first seven columns display data from control lysates from HMVECs. The middle seven columns display data from HMVECs in which the α_7 subunit was knocked down and the last set of seven columns display data in which α_9 receptor was knocked down. Within each set of columns, there is a time course from 0 to 60 min. Yellow denotes increased staining and blue denotes decreased staining compared to the control HMVEC lysate at the 0 time point. The intensity of the color reflects the magnitude of the change from baseline. The dendrogram on the left of matrix represents similarities in patterns of activity among phosphoproteins. C,D: Corresponding immunoblots for the phosphoproteins in the microarray. [Color figure can be viewed in the online issue, which is available at www.interscience.wiley.com.]

effect of the combination of tobacco smoke and IL-1 β on β-catenin redistribution required the generation of reactive oxygen species and activation of Src/EGFR-p38MAPK, inhibiting PTEN and thereby promoting PI3K/Akt phosphorylation of β-catenin. The activation of this pathway by tobacco smoke was confirmed in the cardio-vascular tissue of ApoE deficient mice. Activation of β-catenin is known to increase endothelial permeability [Barbieri and Weksler, 2007], and could favor pathological processes involved in atherogenesis (accumulation of lipid; entry of immune cells) as well as neovascularization (EC migration and proliferation). We postulate that these effects of tobacco smoke on the vessel wall may be mediated in part by nicotine-induced activation of the endothelial α_7 nAChR.

Previously, we have observed that the expression of the α_7 nAChR subunit is increased in cell culture by hypoxia and by VEGF, known stimuli for angiogenesis. Furthermore, we have previously reported that α-bungarotoxin inhibits EC proliferation, migration and tube formation in vitro. However, this toxin binds to homomeric receptors (both α_7 and α_9 AChRs) as well as the heteromeric nAChR found in the neuromuscular junction. In mice that are homozygous for deficiency of the α_7 AChR, nicotine enhancement of inflammatory angiogenesis is attenuated. Taken together, our findings support the primacy of the endothelial α_7 nAChR in nicotine-mediated angiogenesis, although other nAChR subunits may modulate the effects of nicotine on EC.

Until this report, there had not been a comprehensive characterization and comparison of nAChRs on different endothelial cell types. We find that human endothelial cells express most nAChR subunits, although subunit expression is variable depending upon the origin of the endothelial cells. Of interest, the α_9 nAChR subunit (which also forms homomeric receptors) appears to oppose some of the effects of nicotine mediated by the α_7 nAChR. This observation might be explained by the fact that in neuronal cells, nicotine acts as an antagonist at the α_9 nAChR [Verbitsky et al., 2000]. Nicotine does not activate Ca^{2+} transients in rat GH4C1 pituitary cells transfected with cDNA encoding the α_9 subunit [Fucile et al., 2006]. However, this explanation is not consistent with our finding that siRNA against the α_9 nAChR recapitulated or enhanced the effects of nicotine on NO synthesis, the phosphorylation of multiple signaling proteins, and endothelial cell proliferation. Accordingly, we suspect that endogenous acetylcholine, acting on the α_9 nAChR, opposes the signaling pathway mediated by the α_7 nAChR (Fig. 10). Release of
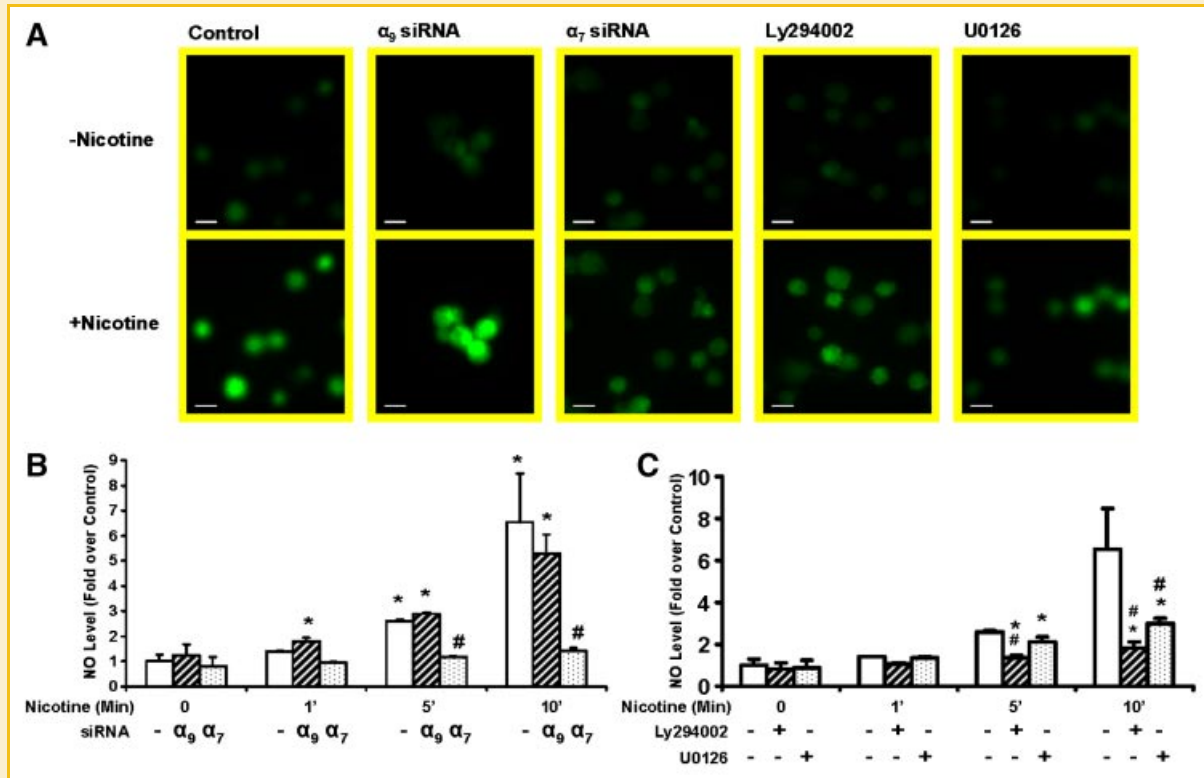
Fig. 8. Nicotine increases NO production. A: HMVECs were loaded with DAF–FM DA (20 μM) as described in Materials and Methods Section. Increasing fluorescence intensity reflects NO synthesis. Representative results are shown. Upper panels show basal fluorescence intensity before stimulation. Bottom panels show fluorescence 15 min after nicotine(10^{-7} M) stimulation. From left to right: Panel 1: Control cells, treated with transfection vehicle for 72 h prior to nicotine stimulation; Panel 2: cells treated with siRNA against α_9 preceding the nicotine stimulation. Panel 3: cells pretreated with siRNA against α_7 prior to nicotine stimulation. Panel 4: cells pretreated with PI3 kinase inhibitor Ly294003 (50 μM) for 1 h followed by nicotine stimulation. Panel 5: cells pretreated with U0126 (20 μM) for 1 h followed by nicotine stimulation. Bar $= 20\,\mu$m. B,C: Measurement of the intracellular NO level. The average intensities in the ECs relative to the control group were evaluated as described in Materials and Methods Section, n = 10. $^{*}P < 0.05$ versus control (non–transfected) cells at time 0. $^{\#}P < 0.05$ versus non–transfected cells exposed to same stimulus duration. [Color figure can be viewed in the online issue, which is available at www.interscience.wiley.com.]
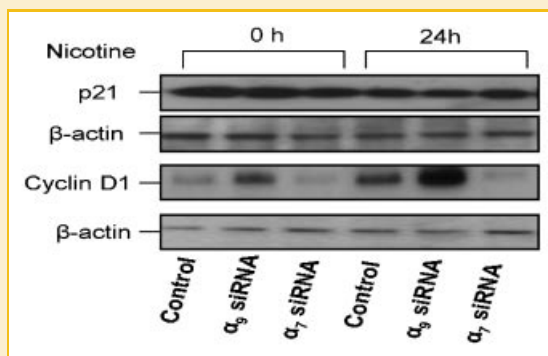

Fig. 9. Cyclin D1 activity is increased by nicotine. Immunoblotting for p21 and cyclin D1. Cells were exposed to siRNA against α_9 or α_7 for 72 h. Then cells were serum starved overnight and subsequently stimulated with nicotine (10^{-10} M) for 24 h. The lysates were subjected to Western analysis with anti–p21, anti–cyclin D1 antibodies. Equal protein loading was determined by anti–β–actin antibody.

this tonic suppression by siRNA against the α_9 nAChR, enhances some effects of exogenous nicotine.

Indeed, the α_9 nAChRs were first described as inhibitory receptors in the cochlear and vestibular hair cells [Elgoyhen et al., 1994; Verbitsky et al., 2000; Fuchs, 2002]. There they mediate postsynaptic hyperpolarization and the suppressive effects of the olivocochlear efferent pathway on cochlear responses. However, most recently and in apparent opposition to our findings, Grando's group has observed that the α_9 nAChR plays a critical role in promoting keratinocyte migration [Peng et al., 2004; Chernyavsky et al., 2007]. In this elegant study, they characterized the role of the α_9 nAChR in the disassembly of cell–cell and cell–matrix interactions. After exposure to siRNA against α_9, the migration of keratinocytes was inhibited; cells became elongated and produced filopodia, but most of them remained anchored to the substrate by long cytoplasmic processes that stretched during migration instead of retracting. Activation of the α_9 nAChR stimulated the phosphorylation of adhesion molecules comprising focal adhesions (FAK, paxillin) and intercellular junctions (β-catenin, desmoglein 3). The signaling cascade induced by α_9 nAChR included activation of phospholipase C, Src, EGFR kinase, protein kinase C, Rac and Rho. Thus it appears that the
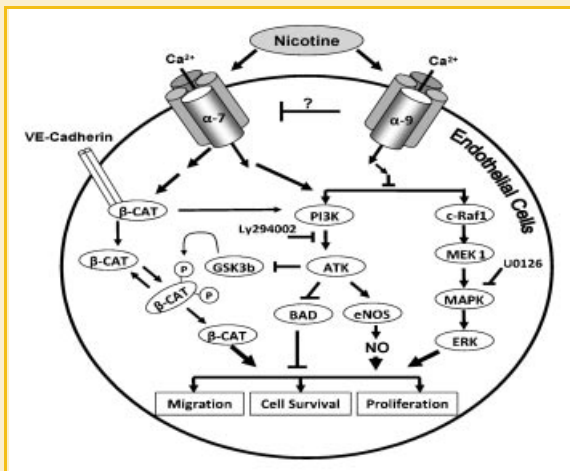
Fig. 10. Schematic representation of nicotine signal transduction pathways. Nicotine activates α_7–nAChRs, triggering an initial cytosolic influx of Ca^{2+}, which activates two major signaling pathways (PI3/Akt and MAPK cascade, respectively) resulting in the promotion of cell proliferation, survival and migration. The activation of MAPK and Akt increases NO synthesis, which also promotes EC proliferation, survival and migration. Nicotine causes disassembly of the VE–Cadherin/β–catenin complex and translocation of β–catenin to the nucleus. By contrast, nicotine binding to α_9 opposes this signaling pathway through an unknown mechanism.

function and signaling of a specific nAChR is likely to be tissue and context dependent.

The current studies indicate that the α_7 nAChR plays a critical role in EC proliferation, survival, migration and tube formation. These findings are consistent with our previous observation that the α_7 nAChR deficient mouse has an attenuated angiogenic response to nicotine [Heeschen et al., 2002]. The current findings are also consistent with our previous finding that α-bungarotoxin (a selective antagonist of homomeric nAChRs and the neuromuscular nAChR) can inhibit nicotine-induced EC angiogenic processes [Heeschen et al., 2002; Ng et al., 2007; Kiuchi et al., 2008].

By contrast to nicotine, VEGF is a stronger stimulus of angiogenic processes in vitro. In this paper, VEGF appears to induce EC migration more strongly (Fig. 3B). This observation is consistent with our previous work, indicating that VEGF is a stronger activator of EC migration [Ng et al., 2007]. However, it is quite intriguing that siRNA against the α_7 nAChR inhibits VEGF-induced EC migration (Fig. 3B). Similarly, we have previously shown that pharmacological antagonists of the nAChR inhibit VEGF- or FGF-induced EC migration [Ng et al., 2007]. Conversely, nicotine activates many of the same signaling and transcriptional pathways also known to be activated in EC by VEGF and FGF [Heeschen et al., 2002; Ng et al., 2007]. Notably, *in the absence of nicotine*, nAChR antagonists inhibit pathological angiogenesis in pre-clinical models of tumor angiogenesis, choroidal neovascularization, and inflammatory angiogenesis [Heeschen et al., 2002; Kiuchi et al., 2008]. These observations indicate that in setting of pathological angiogenesis, there is a contribution of cholinergic signaling to activate endothelial cells. These observations indicate that in setting of pathological angiogenesis, there is a contribution of cholinergic signaling to activate endothelial cells. Endothelial cells contain all of the

machinery to synthesize and to metabolize acetylcholine, which may then act as a paracrine or autocrine stimulus to reinforce other angiogenic stimuli [Cooke and Ghebremariam, 2008].

To conclude, we find that endothelial cells express most of the known mammalian nAChR subunits. However, the effects of nicotine to enhance endothelial cell proliferation and migration, and its activation of kinase cascades and transcriptional factors, are largely mediated through the α_7 nAChR (Fig. 10). These mechanisms may contribute to pathological neovascularization in tobacco-related diseases, and may have therapeutic relevance.

MATERIALS AND METHODS

CELL CULTURE

We utilized human pulmonary artery endothelial cells (Cascade Biologics, Portland, OR); human retinal microvascular endothelial cells (Cell Systems Inc., Kirkland, WA); human umbilical venous endothelial cells and human dermal microvascular endothelial cells (Cell applications Inc., San Diego, CA or from Cambrex-BioSciences, Walkersville, MD). We grew cells under standard conditions in endothelial cell growth media (Cambrex-BioSciences, Walkersville, MD). Reagents included nicotine (free base; Sigma–Aldrich, St. Louis, MO). We used monoclonal antibodies against: β-Catenin (BD Biosciences, San Jose, CA); active-β-catenin (Upstate, Lake Placid, NY); phospho-Erk1/2, p21, cyclinD1, phospho-Akt, phospho-eNOS (Cell signaling, Beverly, MA);, α_7 nAChR (Santa Cruz Biotechnology Inc., Santa Cruz, CA), α_9 nAChR (Aviva Biosystems, San Diego, CA), and β-actin (Sigma–Aldrich).

CELL MIGRATION ASSAY

In this model a region of a confluent EC monolayer is mechanically removed, and over the following days cells from the intact area of the monolayer migrate into the denuded area [Herman, 1993]. For this assay we employed a confluent monolayer of early passage ($P < 7$) HMVEC. Angiogenic factors or vehicle were added in the following concentrations: nicotine (10^{-8} M) or VEGF (10 ng/ml). The extent of migration was quantified by counting the number of cells mobilized into the denuded area for a total of 12 microscopic fields of view ($10\times$) per 60 mm plate. All migration assays were performed by individuals blinded to treatment conditions and repeated using at least three independent vials of primary cells, with each experiment reproduced at least in triplicate.

CELL PROLIFERATION ASSAY

Cell proliferation assay was performed using ABSULUTE-S SBIP cell proliferation assay kit (Molecular Probes, Invitrogen, CA). HMVEC were cultured on 60 mm tissue plate and serum free for overnight. After treated with or without growth factor for 6 h, 6 μl BrdU photolyte stock solution was added to the culture dish and further incubated for 40 min. Cells were then harvested and subjected to photolysis of DNA and TUNEL assay as instructed by company's protocol. Analysis was performed by flow cytometry on FACS Scan (BD Biosciences).

CELL APOPTOSIS ASSAY

The cell apoptosis assay was performed using an Annexin V apoptosis assay kit (Molecular Probes). Firstly, subconfluent HMVECs were transfected with $\alpha7$, $\alpha9$, or scrambled siRNA. Seventy-two hours after the transfection, confluent HMVECs were exposed to serum free conditions overnight then cultured in EBM for 24 h, with or without nicotine. Cells were harvested and incubated with Annexin V according to manufacturer's protocol. The cell samples were analyzed by flow cytometry on FACS Scan (BD Biosciences).

MATRIGEL IN VITRO TUBE FORMATION ASSAY

A 24-well tissue culture plate was prechilled at $-20°C$ and carefully coated with growth factor-reduced Matrigel (BD Biosciences, Bedford, MA) in 400-μl/well volumes and allowed to solidify for 30 min at $37°C$. After the Matrigel solidified, 1×10^5 HMVEC were suspended in 1 ml of EC medium and added to individual Matrigel-coated wells. The cells were then incubated at $37°C$ for 6 h and observed for tubulogenesis. Images were captured using phase-contrast microscopy at $20\times$ magnification using a CCD camera and analyzed using Spotfire software. For quantification of the angiogenic response, the length of individual tubes were measured by drawing a line along each tube and measuring the length of the line in pixels then calibrating with a micrometer present in the image. Tube length was measured in five non-overlapping fields under $20\times$ magnification.

GENE SILENCING BY SMALL INTERFERING RNAs (siRNAs)

Four pairs of double-stranded siRNA against each nAChR subunit were designed using siRNA Target finder software from Ambion and synthesized at Stanford core facility (PAN, Stanford University) for selective silencing of nAChR subunits. The siRNAs were transfected into cells with HiPerFect (Qiagen, Valencia, CA). The sequence of siRNA utilized in the experiments shown are: α-5 (UCCUCUG-CUGGCAGUACUUdtt), α-6 (AUUGCGCUGGGAUCCAAUGdtt), α-7 (UGACUCGCAACCACUCACCdtt), α-9 (UGUGACCCUGCAGAUUA-CGdtt),α-10 (GCUGUUCCGUGACCUCUUUdtt), β-2 (UGCCGUGGU-CUCCUAUGAUdtt), β-3 (ACGGAACUGUUGUCUGGACdtt), β-4 (UGGACUGAUUACCGCCUGAdtt). Inhibition of each individual nAChR subunit mRNA expression was verified by real-time PCR, and inhibition of protein expression was verified by Western blot analysis where specific commercial antibodies were available. Based upon their efficacy in reducing mRNA and protein expression, one of the four pairs of siRNA that successfully knocked down the subunit mRNA was selected for each nAChR subunit. Scrambled (randomly arranged) siRNA or transfection vehicle alone were used as controls for the transfection process and any non-specific effects of the siRNA.

REAL-TIME RT-PCR ANALYSIS OF nAChR SUBUNITS

The mRNA levels for nAChR isoforms were measured using a real-time reverse transcriptase polymerase chain reaction (RT-PCR) assay. Total RNA was extracted from cultured cells using the RNeasy® Mini Kit (Qiagen, Valencia, CA). Assays-on-Demand primers and probes (Applied Biosystems, Foster City, CA) for the human genes of the nAChR subunits $\alpha1$, $\alpha2$, $\alpha3$, $\alpha4$, $\alpha5$, $\alpha6$, $\alpha7$, $\alpha9$, $\alpha10$, $\beta1$, $\beta2$, $\beta3$ and $\beta4$, δ, ε and γ were used for One-Step Real Time PCR using TaqMan One-Step RT-PCR master Mix Reagents Kit (Applied Biosystems). Amplification was performed on ABI 7300 Real time PCR System. The data from triplicate samples were analyzed with the sequence detector software (Applied Biosystems) and expressed as mean ($\pm$SEM) of mRNA relative to that of 18S RNA. Fold induction over control is determined by normalizing treated samples to the control.

MEASUREMENT OF CYTOSOLIC Ca^{2+} LEVELS

Measurements of intracellular Ca^{2+} were made in HMVECs in primary cultures. The ECs were pre-seeded in 4-well chamber slides and incubated in 200 μl Fluo-4 solution (Fluo-4 NW calcium assay kits; Invitrogen, CA) for 30 min in $37°C$, and then at room temperature for additional 30 min. Recordings of intracellular Ca^{2+} were made as previously described [Gee et al., 2000]. Images were acquired with a CCD camera, stored and analyzed digitally using ImagePro software. To generate curves of dye fluorescence intensity versus time for cells in culture, we used data from the background-corrected, normalized fluorescence images. Average (per pixel) values were sampled from cellular regions. The same precise sample region for each time point was used for each curve.

MEASUREMENT OF NO LEVEL

To measure the NO level in ECs, serum starved ECs were loaded with 4-amino-5-methylamino-$2'$,$7'$-difluorofluorescein diacetate (DAF-FM DA, 10 μM, Invitrogen, CA) for 60 min at $37°C$ and stimulated with nicotine(10^{-7} M). NO was visualized as green under laser microscopy. Images were acquired with a CCD camera, stored and analyzed digitally under the control of ImagePro software.

PLASMIDS, TRANSIENT TRANSFECTIONS, AND LUCIFERASE ASSAYS

For these studies we used TOPflash, a reporter plasmid containing six TCF binding motifs upstream of a minimal TK promoter and the firefly *luciferase* gene (Upstate Biotechnologies, NY); and pRL-TK, containing *Renilla* luciferase under the control of the minimal TK promoter (Promega). HMVEC or PAEC were plated into12-well tissue culture dishes and grown to 60% confluence. Cells in triplicate wells were pre-transfected with siRNA against α_7 or α_9 subunits or scrambled siRNA for 48 h and further transfected with TOPFLASH, or FOPFLASH or pRL-TK. Transfection efficiency, assessed by transfecting cells with 0.8 μg/well Luciferase expression was detected using the Dual Luciferase Reporter Assay System (Promega) with a Turner Luminometer (Turner Designs). Readings for firefly luciferase and *Renilla* luciferase were recorded, and the ratio of firefly to *Renilla* luciferase activity was determined. Assays were performed three times with similar results; a representative experiment is shown. Mean value, SEM, and statistical significance were determined by ANOVA using Prism software.

LYSATE PREPARATION AND RPP MICROARRAY FABRICATION

The RPP microarray studies were performed as described by Chan et al. [2004]. At the end of the incubation period with nicotine, cell lysates were obtained in lysis buffer containing 100 mM Tris–HCl (pH 6.8), 4% SDS (w/v), 10% glycerol (v/v), 2% 2-mercaptoethanol (v/v), 5 mM EDTA, Complete Protease Inhibitor Cocktail (1:5 dilution

of stock solution) (Roche, Indianapolis, IN), and Halt Phosphatase Inhibitor Cocktail (1:16 dilution of stock solution) (Pierce, Rockford, IL) and immediately snap-frozen in a dry ice/ethanol bath. Nicotine treated and control lysate samples were adjusted to contain the same concentration of total protein, as measured using the Quant-iT Protein Assay kit (Invitrogen), before printing. Lysates were then transferred to wells in a 384-well plate and printed in triplicate using a contact-printing VersArray ChipWriter Compact system (Bio-Rad, Hercules, CA) fitted with solid pins. Lysates were arrayed on single-pad nitrocellulose-coated slides (FAST slides; Whatman, Florham Park, NJ). After printing, the slides were dried for 24 h at 23°C before further processing.

RPP MICROARRAY PROCESSING

Microarray slides were assembled into FAST frames and treated with a blocking reagent (Bio-Rad) for 4 h at 23°C. The slides were then probed with primary rabbit or mouse antibodies that recognize either total or phospho-specific proteins (Cell Signaling, Beverly, MA) at 1:1,000 dilution in PBS supplemented with 10% fetal calf serum and 0.1% Tween 20 overnight at 4°C. The slides were washed extensively with PBS-Tween 20 and treated with horseradish peroxidase-conjugated donkey antibody to rabbit or mouse IgG (Jackson ImmunoResearch laboratories) at 1:1,000 dilution for 45 min at 23°C. To amplify the signal, the slides with incubated in 1× Bio-Rad Amplification Reagent supplied in the Amplified Opti-4CM Substrate Kit (Bio-Rad) for 10 min at 23°C. To detect bound biotin, the slides were probed with streptavidin conjugated to Alexa Fluor 647 (Invitrogen) for 1 h at 23°C. A separate slide was probed with a Cy 5 conjugated antibody to β-actin at a 1:2,000 dilution. Stained slides were washed with PBS-Tween 20, rinsed under PBS, and dried under desiccation for a minimum of 1 h before scanning.

IMAGE ANALYSIS AND DATA ACQUISITION

Microarray images were captured at 10-µm resolution with a GenePix 4000B scanner (Molecular Devices, Sunnyvale, CA) using the 635-nm laser and 670DF40 emission filter. GenePix Pro Ver 6.0 (Molecular Devices) was used to determine the median fluorescent intensity of each spot and its surrounding background pixels. The median intensity value

STATISTICAL ANALYSIS

Values for the proliferation and migration activity assays revealed a Gaussian distribution. Hence, comparisons between groups were analyzed by t-test (two-sided) or ANOVA for experiments with more than two groups. Post-hoc range tests and pairwise multiple comparisons were performed with the t-tests (two-sided) with Bonferonni correction.

ACKNOWLEDGMENTS

and the Stanford Cardiovascular Institute. Dr. Cooke is the inventor of patents owned by Stanford University for diagnostic and therapeutic applications of the NOS pathway from which he receives royalties. Dr. Cooke and Dr. Wu are inventors on Stanford University patents related to therapeutic applications of the nAChR pathway for therapeutic modulation of angiogenesis. Several of these patents have been licensed to CoMentis Inc., in which company Dr. Cooke has equity.

REFERENCES

Barbieri SS, Weksler BB. 2007. Tobacco smoke cooperates with interleukin-1beta to alter beta-catenin trafficking in vascular endothelium resulting in increased permeability and induction of cyclooxygenase-2 expression in vitro and in vivo. FASEB J 21:1831–1843.

Barbieri SS, Ruggiero L, Tremoli E, Weksler BB. 2008. Suppressing PTEN activity by tobacco smoke plus interleukin-1 β modulates dissociation of VE-cadherin/β-catenin complexes in endothelium. Arterioscler Thromb Vasc Biol 28:732–738.

Behrens J, von Kries JP, Kahl M, Bruhn L, Wedlich D, Grosschedl R, Birchmeier W. 1996. Functional interaction of beta-catenin with the transcription factor LEF-1. Nature 382:638–642.

Boulter J, Connolly J, Deneris E, Goldman D, Heinemann S, Patrick J. 1987. Functional expression of two neuronal nicotinic acetylcholine receptors from cDNA clones identifies a gene family. Proc Natl Acad Sci USA 84:7763–7767.

Chan SM, Ermann J, Su L, Fathman CG, Utz PJ. 2004. Protein microarrays for multiplex analysis of signal transduction pathways. Nat Med 10:1390–1396.

Chan SM, Weng AP, Tibshirani R, Aster JC, Utz PJ. 2007. Notch signals positively regulate activity of the mTOR pathway in T-cell acute lymphoblastic leukemia. Blood 110:278–286.

Chernyavsky AI, Arredondo J, Vetter DE, Grando SA. 2007. Central role of alpha9 acetylcholine receptor in coordinating keratinocyte adhesion and motility at the initiation of epithelialization. Exp Cell Res 313:3542–3555.

Cooke JP. 2007. Angiogenesis and the role of the endothelial nicotinic acetylcholine receptor. Life Sci 80:2347–2351.

Cooke JP, Ghebremariam Y. 2008. Endothelial nicotinic acetylcholine receptors and angiogenesis. Trends in Cardiovascular Medicine 18:247–253.

Cooke JP, Losordo DW. 2002. Nitric oxide and angiogenesis. Circulation 105:2133–2135.

Dasgupta P, Chellappan SP. 2006. Nicotine-mediated cell proliferation and angiogenesis: New twists to an old story. Cell cycle 5:2324–2328.

Datta SR, Brunet A, Greenberg ME. 1999. Cellular survival: A play in three Akts. Genes Dev 13:2905–2927.

Dejana E. 2004. Endothelial cell-cell junctions: Happy together. Nat Rev Mol Cell Biol 5:261–270.

Dimmeler S, Fleming I, Fisslthaler B, Hermann C, Busse R, Zeiher AM. 1999. Activation of nitric oxide synthase in endothelial cells by Akt-dependent phosphorylation. Nature 399:601–605.

Elgoyhen AB, Johnson DS, Boulter J, Vetter DE, Heinemann S. 1994. Alpha 9: An acetylcholine receptor with novel pharmacological properties expressed in rat cochlear hair cells. Cell 79:705–715.

Folkman J. 1995. Angiogenesis in cancer, vascular, rheumatoid and other disease. Nat Med 1:27–31.

Fradin M, Gammeltoft S. 1999. Role and regulation of 90 kDa ribosomal S6 kinase (RSK) in signal transduction. Mol Cell Endocrinol 151:65–77.

Fuchs P. 2002. The synaptic physiology of cochlear hair cells. Audiol Neuro-otol 7:40–44.

Fucile S. 2004. Ca2+ permeability of nicotinic acetylcholine receptors. Cell Calcium 35:1–8.

Fucile S, Sucapane A, Eusebi F. 2006. Ca2+ permeability through rat cloned alpha9-containing nicotinic acetylcholine receptors. Cell Calcium 39:349–355.

Gee KR, Brown KA, Chen WN, Bishop-Stewart J, Gray D, Johnson I. 2000. Chemical and physiological characterization of fluo-4 Ca(2+)-indicator dyes. Cell Calcium 27:97–106.

Gotti C, Moretti M, Gaimarri A, Zanardi A, Clementi F, Zoli M. 2007. Heterogeneity and complexity of native brain nicotinic receptors. Biochem Pharmacol 74:1102–1111.

Grando SA, Kawashima K, Kirkpatrick CJ, Wessler I. 2007. Recent progress in understanding the non-neuronal cholinergic system in humans. Life Sci 80:2181–2185.

Guo M, Wu MH, Granger HJ, Yuan SY. 2004. Transference of recombinant VE-cadherin cytoplasmic domain alters endothelial junctional integrity and porcine microvascular permeability. J Physiol 554:78–88.

Hay N. 2005. The Akt-mTOR tango and its relevance to cancer. Cancer Cell 8:179–183.

Heeschen C, Jang JJ, Weis M, Pathak A, Kaji S, Hu RS, Tsao PS, Johnson FL, Cooke JP. 2001. Nicotine stimulates angiogenesis and promotes tumor growth and atherosclerosis. Nat Med 7:833–839.

Heeschen C, Weis M, Aicher A, Dimmeler S, Cooke JP. 2002. A novel angiogenic pathway mediated by non-neuronal nicotinic acetylcholine receptors. J Clin Invest 110:527–536.

Herman IM. 1993. Molecular mechanisms regulating the vascular endothelial cell motile response to injury. J Cardiovasc Pharmacol 22(Suppl 4): S25–S36.

Ilan N, Tucker A, Madri JA. 2003. Vascular endothelial growth factor expression, beta-catenin tyrosine phosphorylation, and endothelial proliferative behavior: A pathway for transformation? Lab Invest 83:1105–1115.

Kiuchi K, Matsuoka M, Wu JC, Silva RL, Kengatharan K, Verghesa M, Ueno S, Yokoi K, Khu N, Cooke JP, Campochiaro PA. 2008. Mecamylamine suppresses basal and nicotine-stimulated choroidal neovascularization. Invest Ophthalmol Vis Sci 49:1705–1711.

Kojima H, Nakatsubo N, Kikuchi K, Kawahara S, Kirino Y, Nagoshi H, Hirata Y, Nagano T. 1998. Detection and imaging of nitric oxide with novel fluorescent indicators: Diaminofluoresceins. Anal Chem 70:2446–2453.

Lips KS, Pfeil U, Kummer W. 2002. Coexpression of alpha 9 and alpha 10 nicotinic acetylcholine receptors in rat dorsal root ganglion neurons. Neuroscience 115:1–5.

Morgan DO. 1995. Principles of CDK regulation. Nature 374:131–134.

Ng MKC, Wu J, Chang E, Wang B-y, Katzenberg-Clark R, Ishii-Watabe A, Cooke JP. 2007. A central role for nicotinic cholinergic regulation of growth factor-induced endothelial cell migration. Arterioscler Thromb Vasc Biol 27:106–112.

Obaya AJ, Sedivy JM. 2002. Regulation of cyclin-Cdk activity in mammalian cells. Cell Mol Life Sci 59:126–142.

Peng H, Ferris RL, Matthews T, Hiel H, Lopez-Albaitero A, Lustig LR. 2004. Characterization of the human nicotinic acetylcholine receptor subunit alpha (alpha) 9 (CHRNA9) and alpha (alpha) 10 (CHRNA10) in lymphocytes. Life Sci 76:263–280.

Shesely EG, Maeda N, Kim HS, Desai KM, Krege JH, Laubach VE, Sherman PA, Sessa WC, Smithies O. 1996. Elevated blood pressures in mice lacking endothelial nitric oxide synthase. Proc Natl Acad Sci USA 93:13176–13181.

Verbitsky M, Rothlin CV, Katz E, Elgoyhen AB. 2000. Mixed nicotinic-muscarinic properties of the alpha9 nicotinic cholinergic receptor. Neuropharmacology 39:2515–2524.

Villablanca AC. 1998. Nicotine stimulates DNA synthesis and proliferation in vascular endothelial cells in vitro. J Appl Physiol 84:2089–2098.

Zhang B, Luo S, Dong X-P, Zhang X, Liu C, Luo Z, Xiong W-C, Mei L. 2007. Beta-catenin regulates acetylcholine receptor clustering in muscle cells through interaction with rapsyn. J Neurosci 27:3968–3973.

Zhu B-q, Heeschen C, Sievers RE, Karliner JS, Parmley WW, Glantz SA, Cooke JP. 2003. Second hand smoke stimulates tumor angiogenesis and growth. Cancer Cell 4:191–196.